Electro-oxidation of Formic Acid at Binary Platinum and Gold Nanoparticle-Modified Electrodes: Effect of Chloride Ions

Gumaa A. El-Nagar[1], Ahmad M. Mohammad[1,2,*], Mohamed S. El-Deab[1,2], Bahgat E. El-Anadouli[1,*]

[1]Chemistry Department, Faculty of Science, Cairo University, Cairo 12613, Egypt
[2]Department of Chemical Engineering, Faculty of Engineering, The British University in Egypt, Cairo 11837, Egypt
[*]E-mail: ammohammad@cu.edu.eg; bahgat30@yahoo.com

The modification of a glassy carbon (GC) electrode with platinum (PtNPs) and gold (AuNPs) nanoparticles was intended to fabricate efficient anodes for the formic acid electro-oxidation (FAO). A suitable deposition sequence of PtNPs and AuNPs was adjusted to enhance the electrocatalytic activity of the electrode in such a way suppressing the CO poisoning that usually deteriorates the electrode's catalytic activity during FAO. Morphologically, PtNPs were deposited in a spherical shape (with an average diameter of 37 nm), while AuNPs appeared in granules (with an average diameter of 43 nm) both were uniformly dispersed on the GC surface. The highest electrocatalytic activity was obtained at the Au-Pt/GC electrode (for which PtNPs was deposited first on the GC electrode then AuNPs). Interestingly, AuNPs could successfully interrupt the contiguity of Pt surface sites in a way preventing the CO poisoning. Moreover, the Au-Pt/GC electrode exhibited excellent tolerance against poisoning influenced by chloride ions, which usually contaminate the fuel cell and have a similar impact as CO. The relationship between the degree of electrode's tolerance against the catalytic deactivation and the chloride ion concentration was addressed.
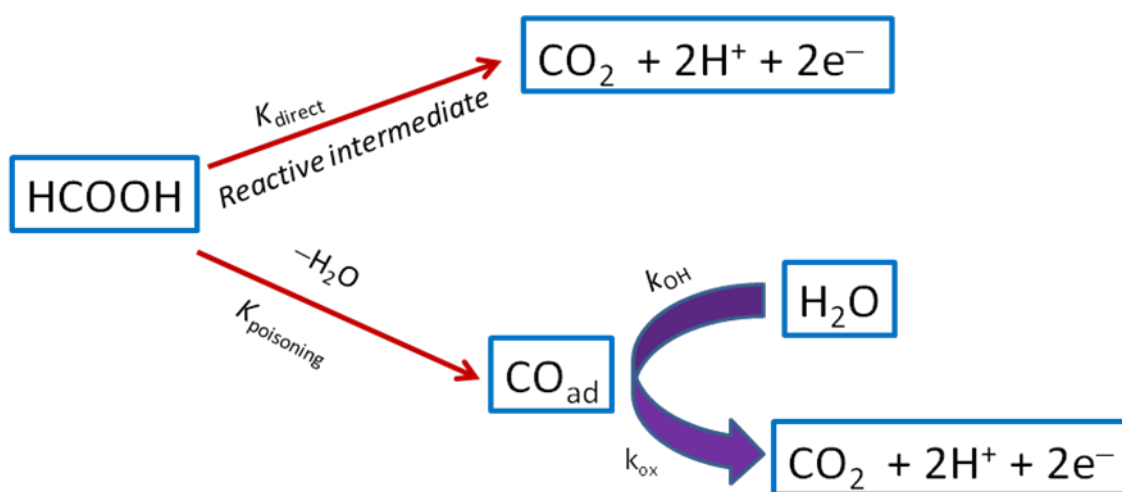
1. INTRODUCTION

Electrocatalysis at nanoparticles-based materials has been a subject of continuously growing interest, particularly for the applications of energy production. Fuel cells (FCs) represent a unique entry into the field of clean, noiseless, incessant, eco-friendly and efficient energy resources. They are progressively replacing the fossil fuels to meet the growing infinite needs of electric power in industry and daily-live activities. In this regard, the direct formic acid fuel cells (DFAFCs) have shown superiority over the traditional hydrogen (HFCs) and direct methanol (DMFCs) fuel cells in providing

electricity for portable electronic devices. While HFCs are limited by difficulties with hydrogen storage and transportation, the DMFCs suffer from the inherent toxicity, and the slow oxidation kinetics of methanol as well as its high crossover through Nafion-based membranes. On the other hand, formic acid (FA) exhibits a smaller crossover flux through Nafion membrane than methanol, allowing the use of high concentrated fuel solutions and thinner membranes in DFAFCs [1-3]. This is highly desirable for the design of compact portable power systems. Furthermore, DFAFCs have a higher theoretical open-circuit potential (1.40 V) than that of hydrogen fuel cells (1.23 V) and DMFCs (1.21 V) and less poisoning impact to platinum-based electrocatalysts than that of methanol [1-7]. Nevertheless, DFAFCs experience a severe problem where the catalytic activity of the Pt anodes, on which the FA electro-oxidation (FAO) proceeds, ceases with time. This is due to the accumulation of the poisoning CO intermediate resulting from the *"non-faradaic"* dissociation of FA. This ultimately deteriorates the overall performance of DFAFC [6,7]. Therefore, the development of efficient and stable anodes overcoming the CO poisoning for FAO is a central issue.

The FAO on Pt follows a dual pathway mechanism (direct and indirect, see Scheme 1). The direct (desirable) route proceeds with the dehydrogenation of FA to CO_2 at low anodic potential (with a peak current I_p^d). Whereas, the indirect (dehydration/undesirable) pathway involves the adsorption of CO at low potential domain and its subsequent oxidation at a higher potential (with a peak current I_p^{ind}) [3,8-10]. The adsorption of CO in the low potential domain blocks the active sites of Pt and thus impedes the oxidation of FA via the direct pathway. In an attempt to overcome the CO poisoning, transition metal oxide nanostructures were deposited on Pt electrodes to mitigate poisoning by facilitating the oxidative removal of CO at relatively low anodic potentials [3]. Alternatively, interrupting the contiguity of the Pt surface atoms could help in this regard, in which a second modifier can effectively decrease the binding strength of CO to the underlying Pt substrate [11-14].

Scheme 1. General mechanism of formic acid electro-oxidation at Pt-based materials

Another serious issue challenging the commercialization of FCs is the electrolyte's contamination with species of a high adsorption tendency, such as chlorides. It should be mentioned

that, most of the high-surface area FCs catalysts are often synthesized from halide-containing educts [15-17], which are not always removed completely after synthesis. Alternatively, chloride is also a likely contaminant in water contained in the feed-streams of fuel cells. Actually, the specific adsorption of chloride can dramatically affect the kinetics of small organic molecules oxidation and oxygen reduction [18-25]. Herein, a simple procedure for the modification of glassy carbon (GC) electrode with gold (AuNPs) and platinum (PtNPs) nanoparticles is introduced for using as an electrocatalyst for FAO. The minute amount of deposited AuNPs could fortunately interrupt the contiguity of the Pt surface sites to increase the electrode' tolerance against the CO poisoning and thus improve the catalytic activity towards FAO. The influence of chloride ions contamination on the catalytic activity of the binary catalyst towards FAO is also investigated.

2. EXPERIMENTAL

GC (d = 3.0 mm) and Pt electrodes (d = 1.6 mm) are used as the working electrodes. The electrodes were cleaned before use by polishing with aqueous slurries of successively finer alumina powder with the help of a microcloth. The Pt electrode was further cleaned by scanning the potential between the onset potential of the hydrogen and oxygen evolution reactions in 0.5 M H_2SO_4 for several cycles until a CV of a clean Pt surface was obtained. A spiral Pt wire and Ag/AgCl/KCl(sat) were used as the counter and reference electrodes, respectively. The electrodeposition of AuNPs on the bare GC and on PtNPs modified GC (Pt/GC) electrodes was carried out in 0.1 M H_2SO_4 containing 1.0 mM $K[AuCl_4]$ solution, and the potential was cycled between 0 and 1.1 V vs. Ag/AgCl/KCl(sat) at 100 mV s^{-1} for 15 cycles. On the other hand, the electrodeposition of PtNPs on the bare GC and on AuNPs modified GC (Au/GC) electrodes was achieved in 0.2 M H_2SO_4 containing 1.0 mM H_2PtCl_6 solution via a constant potential electrolysis at 1 V vs. Ag/AgCl/KCl(sat) for 300 s. All of the chemicals used in this investigation were of analytical grade and used without further purification. The electrochemical measurements were performed at room temperature (25 ± 1°C) in a conventional two-compartment three-electrode glass cell using an EG&G potentiostat (model 273A) operated with Echem 270 software. A field emission scanning electron microscope (FE-SEM, QUANTA FEG 250) coupled with an energy dispersive X-ray spectrometer (EDX) unit was employed to evaluate the electrode's morphology and composition. The electrocatalytic activity of the modified electrodes toward FAO was examined in a solution of 0.3 M FA at pH of 3.5 (the pH was adjusted by adding a proper amount of NaOH). Current densities were calculated on the basis of the real surface area of the working electrode.

3. RESULTS AND DISCUSSIONS

3.1. Materials characterization:

Figure 1A shows the SEM image of the Pt/GC electrode, which signifies the deposition of well-separated PtNPs in a spherical shape with an average particle size of 37 nm. Alternatively, Fig. 1B shows the SEM image for the binary modified GC catalyst (Au-Pt/GC), in which the PtNPs are first electrodeposited on the GC electrode then AuNPs. The deposition of AuNPs on top of the PtNPs

modified GC electrode occurred in grain-like structure (average diameter = 43 nm) that homogeneously covered the entire surface of the GC electrode. The elemental analysis for the Au-Pt/GC electrode is disclosed by EDX (see inset of Fig. 1B). It provides a direct evidence for the successful deposition of Pt and Au particles onto the surface of GC.

3.2. Electrochemical characterization

The electrochemical characterization is a powerful and sensitive technique that is frequently used to identify and distinguish traces from the active ingredients. Figure 2 shows the cyclic voltammograms (CVs) in 0.5 M H_2SO_4 for (a) Pt/GC, (b) Au/GC, (c) Pt-Au/GC (where AuNPs are first electrodeposited on the GC electrode then PtNPs), and (d) Au-Pt/GC electrodes. Figure 2a clearly displays the typical characteristic behavior of a clean polycrystalline Pt surface in acidic medium; the hydrogen adsorption/desorption peaks in the potential range from −0.2 to 0.1 V along with the Pt/PtO transformation peaks at ca. 0.5 V. Similarly, Fig. 2b reflects the typical response characterizing a clean polycrystalline Au surface with the Au oxidation at ca. 1.2 V and its subsequent reduction at ca. 0.9 V. By the way, the bare GC electrode has no characteristic peaks in this potential window [26,27].
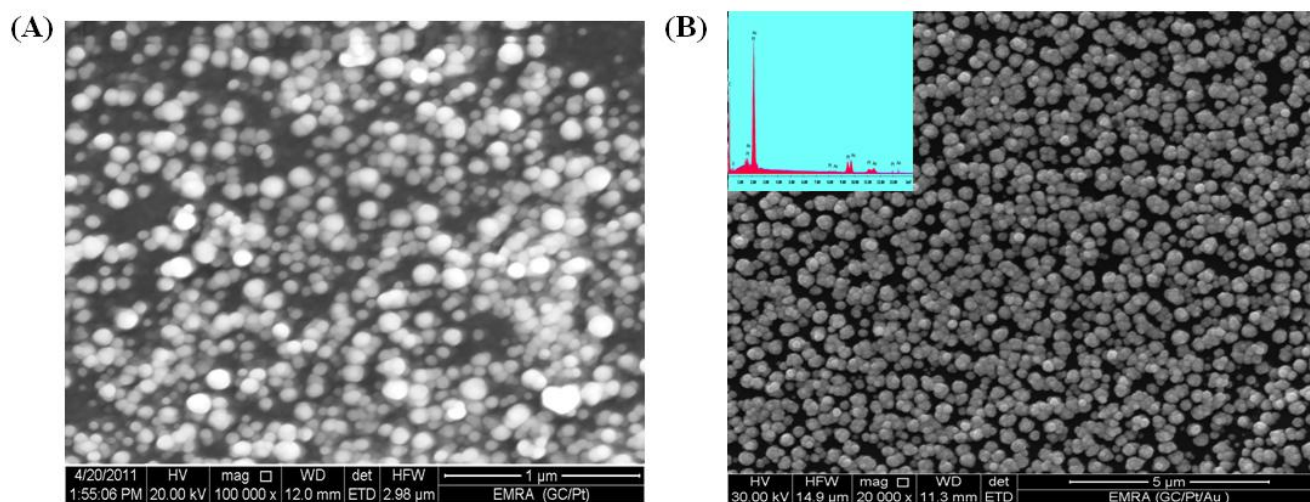

Figure 1. FE-SEM images for (A) Pt/GC and (B) Au-Pt/GC electrodes. Inset of Fig. 1B represents the EDX of the Au-Pt/ GC electrode.

Interestingly, when PtNPs were deposited on the Au/GC electrodes (Fig. 2c), the intensity of the PtO reduction peak (at ca. 0.5 V) increased in comparison to Fig. 2a. This can also be noticed in the Pt oxide formation and the hydrogen adsorption/desorption peaks. This behavior is likely originated from a significant increase in the exposed surface area of Pt. In the Pt-Au/GC electrode, the deposition of AuNPs on the bare GC electrode could eventually increase the available surface sites for the deposition of PtNPs. Hence, the increase in the PtNPs loading in the Pt-Au/GC modified electrode is expected. On the other hand, for the Au-Pt/GC electrode (Fig. 2d), the exposed surface area of Pt

decreased if compared to Fig. 2a. This infers the preferential deposition of AuNPs on top of PtNPs rather than on the bare GC surface. A careful inspection for the Au oxide reduction peak at 0.9 V in the Au/GC, Pt-Au/GC and Au-Pt/GC electrodes (Fig. 1b−d) reveals interesting points. At the Pt-Au/GC modified electrode (Fig. 2c), the Au oxide reduction peak is almost disappeared (note the obvious appearance of the Pt oxide reduction peak). This reveals that AuNPs were almost coated entirely by PtNPs, and what is called a core-shell structure was developed. On the other hand, the appearance of the Au and Pt oxide reduction peaks at the Au-Pt/GC modified electrode (Fig. 2d) suggests the exposure of both of AuNPs and PtNPs at the surface.

Since the electrocatalytic activity towards the FAO depends on the number of available Pt surface sites, the calculation of the real Pt surface area, A_r, will definitely be of great importance. Measurements of the hydrogen adsorption is used to determine A_r [5,13]. Integrating the charge in the potential range from −0.2 to 0.1 V assisted in the estimation of the charge, Q_H (μC), corresponding to the hydrogen adsorption. To obtain A_r from Q_H, we assume that every single hydrogen atom (H_{ad}) is adsorbed on a particular Pt site,
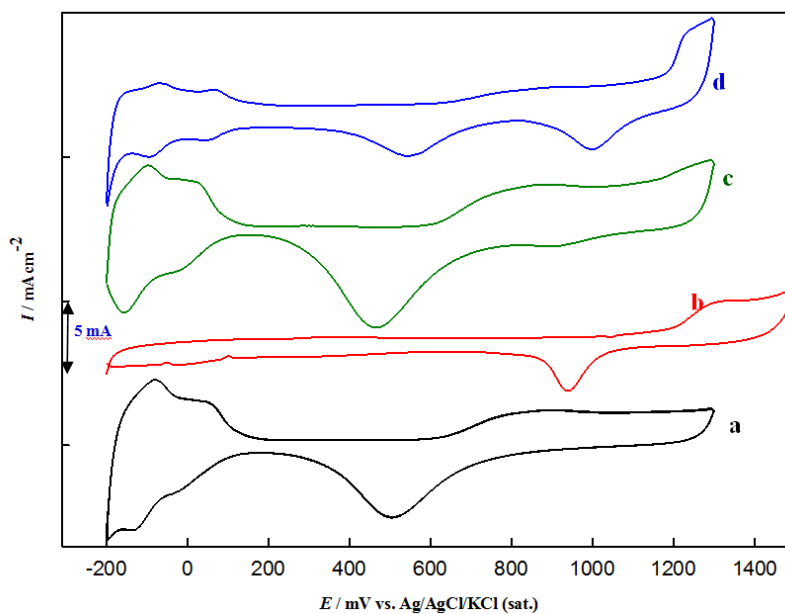
$$H^+ + e^- \rightarrow H_{ad} \tag{1}$$

Figure 2. CVs at 100 mVs^{-1} in 0.5 M H_2SO_4 for (a) Pt/GC, (b) Au/GC, (c) Pt-Au/GC and (d) Au-Pt/GC electrodes

The theoretical charge (Q_0) associated with a monolayer adsorption of hydrogen atoms in 1 cm^2 can be calculated from the following equation:

$$Q_0 (\mu C \ cm^{-2}) = \frac{F \times n}{N} \tag{2}$$

where n represents the number of platinum atoms in 1 cm^2 (ca. 1.3×10^{15} atoms/cm^2), F is the Faraday's constant (9.6×10^4 C mol^{-1}), and N is Avogadro's constant [5]. With these data, Q_0 has been commonly taken as 210 µC/cm^2. Next, A_r (cm^2) is obtained from the charge of hydrogen adsorption as:

$$A_r = \frac{Q_H}{Q_0} \tag{3}$$

The specific surface area S (cm^{2}g^{-1}) of Pt was also estimated as follows [5]:

$$S = \frac{100 A_r}{W_{Pt} A_g} \tag{4}$$

where A_g represents the geometric surface area ($A_g = 0.07$ cm^2) of Pt and W_{Pt} (g) the platinum loading [5], which is obtained from:

$$W_{Pt} = \frac{Q_d M}{zF} \tag{5}$$

where Q_d represents the charge associated with the Pt deposition, M is the atomic mass of platinum (195.09 g mol^{-1}), and z is the number of electrons (= 4) consumed in the reduction of Pt^{4+} ions.

Assuming spherical particles of similar radius for Pt particles, an average particle size of Pt (nm) can be calculated utilizing the procedure of Gloaguen et al [5]:

$$d = \frac{6000}{\rho S} \tag{6}$$

where ρ is the density of platinum (21.4 g cm^{-3}) and S is its specific surface area (cm^{2}g^{-1}). The particle size of PtNPs in the Pt/GC electrode was calculated to be 37 nm, which agrees well with the SEM measurements provided earlier. The real surface areas, platinum loadings, specific surface area and particle size of Pt in the investigated set of electrodes are displayed in Table 1.

Table 1. Physical characteristics of the investigated electrodes.

Electrodes	True surface area, A_r (cm^2)[b]	Pt loading W(mg cm^{-2})	Relative surface area(A_r/A_g)[a]	Specific surface area S (m^2 g^{-1})	Particle size d (nm)
Bulk Pt	0.095	Bulk Pt	1.4	-	-
Pt/GC	0.413	0.085	5.9	7.50	37
Pt-Au/GC	0.871	0.232	13	6.50	43
Au-Pt /GC	0.392	0.093	5.6	5.89	48

a Real surface area (A_r) / geometric surface area (A_g).
b As determined from hydrogen adsorption

3.3. Electrocatalytic oxidation of FA

Figure 3A shows the linear sweep voltammograms (LSVs) in the forward (anodic) direction of FAO at several electrodes in an aqueous solution of 0.3 M FA (pH = 3.5). A typical oxidation behavior for FAO appeared at the bare Pt substrate (curve a) and Pt/GC (curve b) electrodes, with two oxidation peaks at ca. 0.25 V and 0.65 V, respectively. The first oxidation peak (at ca. 0.25 V) is assigned for the direct oxidation of formic acid to CO_2, while the second one (at ca. 0.65 V) is assigned to the oxidation of the adsorbed poisoning CO (CO_{ad}, produced from the *"non-faradaic"* dissociation of FA) to CO_2.
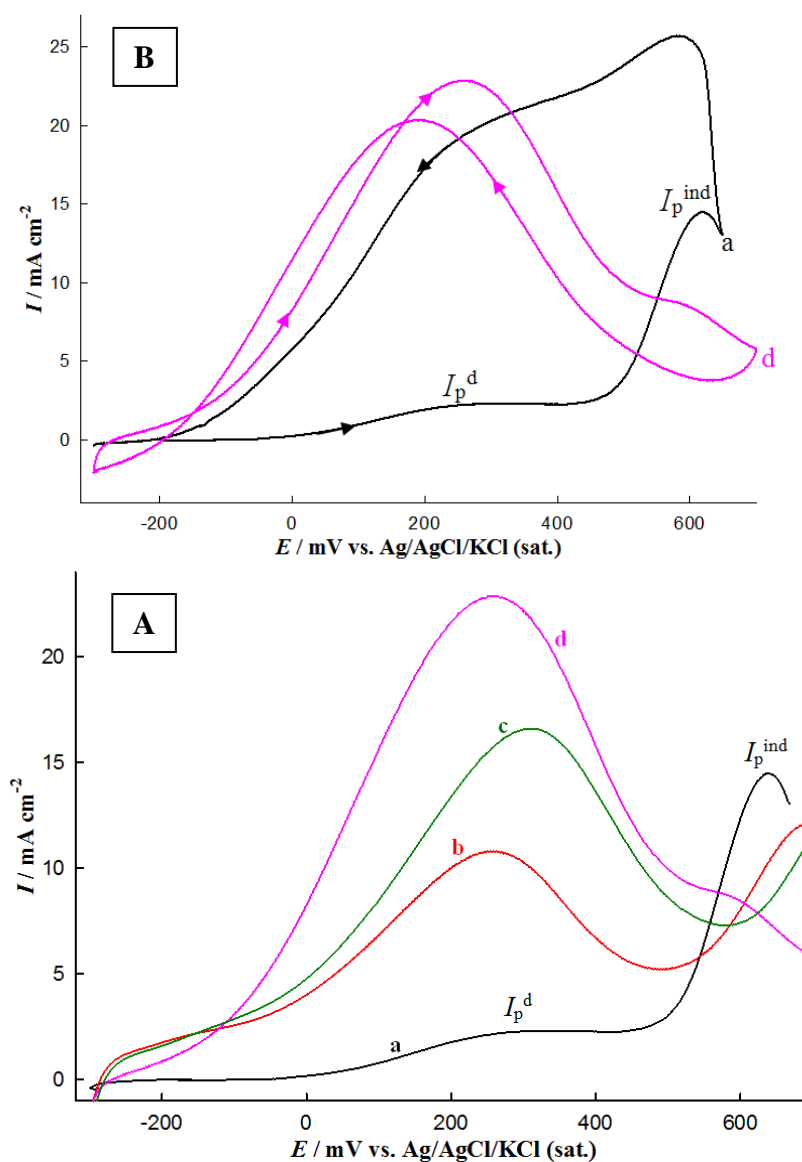

Figure 3. (A) The LSV in 0.3M HCOOH (pH = 3.5) of (a) bare Pt, (b) Pt/GC, (c) Pt-Au/GC and (d) Au-Pt/GC modified electrodes at 100 mVs^{-1}. (B) CVs of FAO for curves a and d of Fig. 3A. Real surface area is employed in calculating the current density.

At low potential domain (ca. 0.25 V), the Pt sites are partially poisoned by CO_{ad} from the dissociative adsorption step. The measured current then mainly comes from the FAO at the free Pt active sites through the direct dehydrogenation pathway. The peak current intensity in this potential range indicates either the density of Pt active sites and/or the poisoning level of Pt surface by CO_{ad}. At a high potential region (ca. 0.65 V), CO_{ad} is oxidized by Pt-OH species that starts to be formed around 0.5 V, which releases most Pt sites for FAO. During the backward scan, similar peaks have appeared and assigned to the same reactions but with a higher catalytic activity (see Fig. 3B). This increase in the catalytic activity is expected as the Pt surface has become relatively free from most of the CO_{ad} and the Pt surface has mostly become hydroxylated Pt–OH_{ad} [3,13,14].

We wish here to emphasize that the adsorption of CO on Pt surface requires the existence of three adjacent Pt sites (with a definite atomic spacing), and any interruption in this continuity may impede its adsorption. In this regard, the modification of Pt/GC substrate with AuNPs has been achieved in two ways. The first involved the direct electrodeposition of AuNPs on the GC surface then PtNPs were next deposited (Pt-Au/GC). The other involved the electrodeposition of PtNPs on the GC substrate then AuNPs (Au-Pt/GC). The role of depositing AuNPs was solely to interrupt the contiguity of the Pt surface atoms which is required for CO adsorption. It is worth mentioning that neither Au nor GC supports the FAO under these experimental conditions simply because the poor adsorption of FA on them [3]. The LSV of the FAO in 0.3 M FA (pH = 3.5) at the Pt-Au/GC and Au-Pt/GC electrodes are depicted in Fig. 3A (curves c and d, respectively). As obviously seen in curve c of Fig. 3A, there was a significant increase in the direct peak of FAO along with a decrease in the indirect peak current if compared to curves a and b (Fig 3A). This can be understood in terms of the large increase in the surface area of Pt which provided plenty of Pt active sites for the participation in the direct route of FAO. This agrees with the data of Fig. 2 which highlighted the significant increase of Pt surface area for the Pt-Au/GC electrode. In parallel, the deposition of AuNPs underneath PtNPs might assist in a geometrical interruption favoring the direct on the expense of the indirect route of FAO. Surprisingly, when the deposition order of AuNPs and PtNPs was reversed (curve d of Fig. 3A), the indirect peak of FAO was completely disappeared with a further increase in the direct peak. Not only that, but the backward oxidation peak current approached the same level of the direct oxidation in the forward scan (see Fig. 3B), in a fashion similar to the ideal behavior reported on Pd. This is really a great achievement to suppress the CO poisoning and to improve the catalytic activity of the direct FAO.

In order to account on the degree of catalytic enhancement towards FAO, two functions are developed; one is the ratio of the current intensities of the direct peak (I_p^d) to the indirect peak (I_p^{ind}), and the second is ratio of I_p^d and the backward direct peak (I_b). The ratio of the two oxidation peaks, I_p^d/I_p^{ind}, (in the anodic sweep direction) reflects the preferential pathway of FAO at a particular electrode. This ratio increased from 0.17 at bare Pt to 1.8 at Pt/GC electrode (*i.e*, about 11 times) which reflects the superiority of PtNPs to bulk Pt for FAO. At the Pt-Au/GC electrode, the (I_p^d/I_p^{ind}) ratio increased to 4.5 (i.e., about 26 times of bare Pt). Surprisingly, at the Au-Pt/GC electrode (θ_{Au} = 65%), the FAO shifted exclusively towards the direct pathway and the I_p^d/I_p^{ind} ratio increased to 146 (i.e., about 859 times compared to bare Pt).

On the other hand, the (I_p^d/I_b) ratio provides useful information about the catalytic tolerance of the electrode against the formation of carbonaceous species. A low I_p^d/I_b ratio indicates poor oxidation

of FA to CO_2 and excess accumulation of carbonaceous species at the electrode surface. This (I_p^d/I_b) ratio increased from 0.09 at bare Pt to 0.91 at Pt-Au/GC electrode. This increase indicates an improvement in catalytic activity of the Pt-Au/GC electrode towards FAO, presumably, via lowering the CO adsorption and favoring the direct oxidation pathway. Interestingly, at the Au-Pt/GC electrode, the ratio I_p^d/I_b was ca. 1.0, indicating a significant tolerance of this electrode against the CO poisoning. This great enhancement in the catalytic activity of this electrode is likely related to the degree of interrupting the contiguity of the Pt sites necessary for CO adsorption [3,13]. The partial deposition of AuNPs on PtNPs (with surface coverage of ~ 65%) in the Au-Pt/GC electrode is believed to work against the CO adsorption, which therefore, decreased the probability of surface poisoning and increased the catalytic activity towards the direct FAO [3, 13].

3.4. Effect of chloride ions

Effort was further dedicated to evaluate the influence of Cl^- ions in the electrolyte of the anodic compartment of DFAFCs, which may act similarly as the poisonous CO, and the degree of tolerance of each electrode against it. Figure 4 shows the LSVs at Pt/GC electrode in 0.3 M FA solution (pH = 3.5) containing (a) 0.0 , (b) 0.5, (c) 1.0, (d) 5, (e) 10, (f) 20, (g) 40 and (h) 50 ppm KCl ions at 100 mV s^{-1}. As clearly seen in Fig. 4 and Table 2, the Cl^- ions influenced the catalytic activity of the electrode towards the FAO, where a decrease in the current density of FAO (I_p^d and I_p^{ind}) was generally observed with the concentration of Cl^- ions. This is very much similar to the deactivation resulted from the CO poisoning, as Cl^- ions have also a great tendency to be adsorbed on Pt surfaces [15-22]. This adsorption consumes partially the active Pt surface available for the FAO.
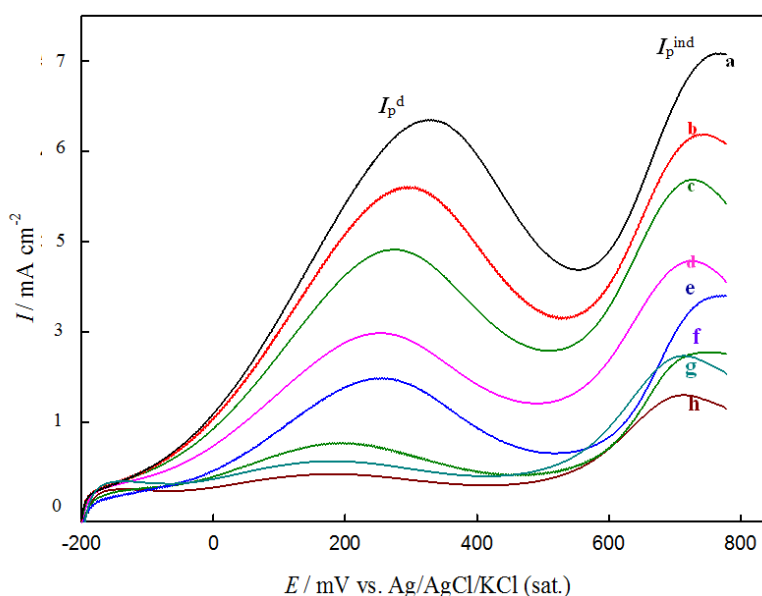

Figure 4. The LSVs (scan rate 100 mVs^{-1}) at Pt/GC electrode in 0.3 M FA solution (pH = 3.5) containing (a) 0.0 , (b) 0.5, (c) 1.0, (d) 5, (e) 10, (f) 20, (g) 40 and (h) 50 ppm of Cl^- ions.

Hence, geometrically, and possibly electronically, the catalytic activity is expected to decrease. The degree of poisoning (can also be inferred from the I_p^d/I_p^{ind} ratio) continued with the Cl$^-$ concentration up to 70 ppm, at which the (I_p^d/I_p^{ind}) ratio decreased to 0.44 (it was 1.8 in absence of Cl$^-$ ions). This lowering in the I_p^d/I_p^{ind} ratio with the Cl$^-$ concentration infers a significant reduction in the catalytic activity of the electrode towards the FAO. Unfortunately, the surface coverage of Cl$^-$ ions on Pt surface increases with the Cl$^-$ concentration, which decreases significantly both of I_p^d and I_p^{ind} but with different rates. At the high potential domain, where the indirect pathway of FAO dominates, the chlorine evolution is expected and the Pt surface is going to retrieve from the Cl$^-$ coverage [22]. This will lead to a difference in the influence of Cl$^-$ concentration on the direct and indirect oxidation currents.

Figure 5 extends the investigation of Cl$^-$ ions impact to FAO at Au-Pt/GC electrode, where the LSVs were recorded at 100 mV s^{-1} in 0.3 M FA solution (pH = 3.5) containing (a) 0.0, (b) 40, (c) 50, (d) 70 and (e) 100 ppm of Cl$^-$ ions. Surprisingly, the Au-Pt/GC electrode was less sensitive to the poisoning effect of Cl$^-$ ions if compared to the Pt/GC electrode (see Fig. 4 and Table 2). For example, 50 ppm Cl$^-$ ions deteriorated the catalytic activity of the Pt/GC electrodes by ca. 80% (compare I_p^d values in Table 2 with respect to the case without Cl$^-$).

Table 2. Effect of [Cl$^-$] on FA oxidation at Pt/GC and Au-Pt/GC electrodes

[Cl$^-$]/ ppm	Pt/GC electrode			Au-Pt/GC electrode		
	I_p^d/ μA	I_p^{ind}/ μA	I_p^d/I_p^{ind}	I_p^d/ μA	I_p^{ind}/ μA	I_p^d/I_p^{ind}
0.0	437	240	1.8	166	1.00	166
10	300	205	1.7	165	1.00	165
20	200	190	1.5	162	1.01	160
30	150	159	1.2	159	0.98	162
40	100	174	0.9	157	0.95	165
50	70.0	139	0.6	155	0.94	164
60	40.0	102	0.4	150	0.92	163
70	29.0	67	0.4	101	0.62	163

The same concentration of Cl$^-$ ions, on the other hand, could reduce the catalytic activity of the Au-Pt/GC electrode only by ca. 6%, and the I_p^d/I_p^{ind} ratio did not change significantly. This is really desirable for fuel cell developers. Figure 6 compares the percent decrease in I_p^d as a function of the Cl$^-$ ions concentration at both of the Pt/GC and Au-Pt/GC electrodes. As obviously seen, the degree of tolerance of the Au-Pt/GC electrode against poisoning with Cl$^-$ ions is much better than that at the Pt/GC electrode at all concentrations of Cl$^-$ ions in the range investigated. Furthermore, the catalytic activity of the Au-Pt/GC electrode was reduced only to ca. 50% in 100 ppm Cl$^-$ ions, while it almost ceased in 50 ppm Cl$^-$ ions at the Pt/GC electrode (see Fig. 6).

We believe the different adsorption tendency of Cl$^-$ ions on Au and Pt is a key to understand this behavior, and soon we will continue the investigation to evaluate the essence of this issue.
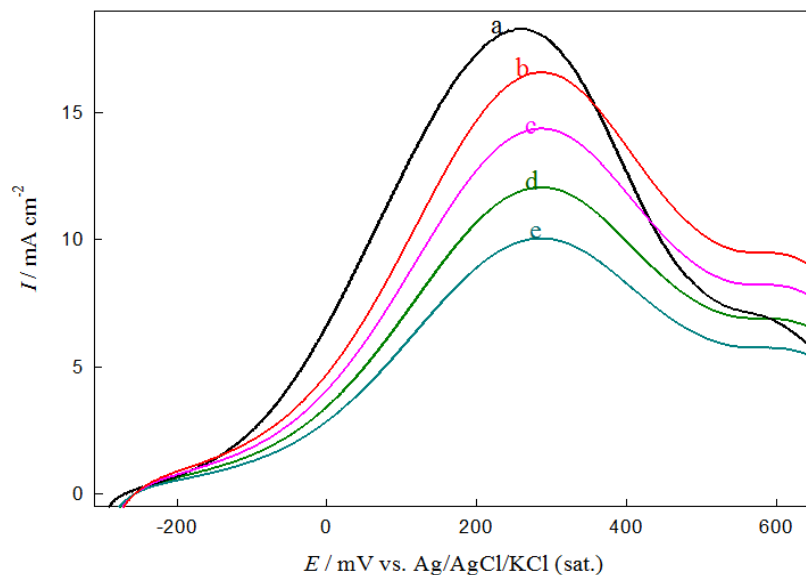
Figure 5. The LSVs at 100 mV s^{-1} obtained at Au-Pt/GC electrode in 0.3 M FA solution (pH= 3.5) containing (a) 0.0, (b) 40, (c)50, (d) 70 and (e)100 ppm Cl^{-} ions.
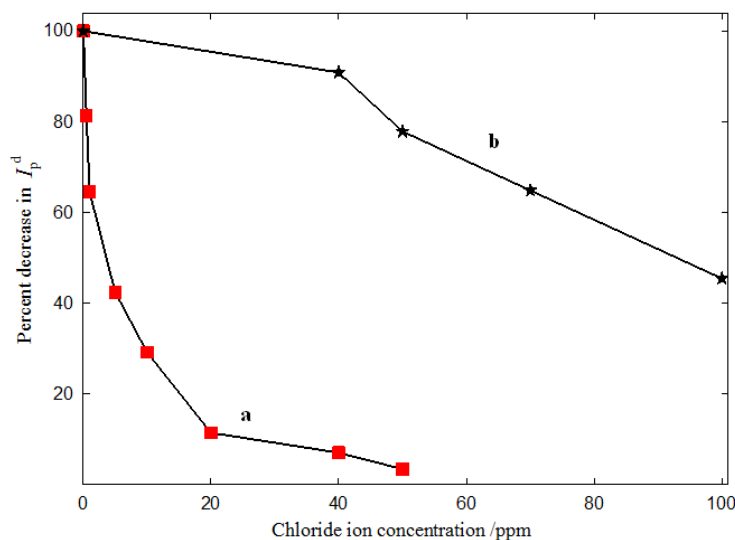

Figure 6. Change of I_p^d for FAO with chloride ion concentration at (a) Pt/GC and (b) Au/Pt/GC. (data were taken from the CVs measured in 0.3 M FA (pH=3.5) at a scan rate of 100 mV s^{-1} in presence of various amounts of chloride ions).

4. CONCLUSION

The current investigation addresses the development of a binary PtNPs and AuNPs catalyst for the efficient FAO. The deposition order of AuNPs and PtNPs was changed and its influence on the catalytic activity towards FAO was revealed. With AuNPs being the topmost layer, the electrocatalytic activity was proved optimum. A mechanistic interpretation for the catalytic activity assumed the necessity of Pt surface sites for the adsorption of FA. The deposition of AuNPs on the Pt/GC electrode interrupted the contiguity of the Pt sites, which is necessary for the CO adsorption. The presence of Cl^{-}

ions led to a decrease in the current density of FAO. The Au-Pt/GC electrode showed an excellent tolerance against the poisoning effect of Cl⁻ than Pt/GC electrode.

References

1. X. Yu and P. G. Pickup, *J. Power Sources,* 182 (2008)124.
2. S. Zhang, Y. Shao, G. Yin and Y. Lin, *J. Power Sources*, 195 (2010) 1103.
3. G. A. El-Nagar, A. M. Mohammad, M. S. El-Deab and B. E. El-Anadouli, *Electrochem. Soc,*. 159 (2012) F249.
4. R. Wang, S. Liao and S. Ji, *J. Power Sources,* 180 (2008) 205.
5. a)B. Habibi and N. Delnavaz, *Int. J. Hydrogen Energy,* 36 (2011) 9581; b) F. Gloaguen, J-M. Leger and C. Lamy, *J. Appl. Electrochem.*, 27 (1997)1052
6. S. Wasmus and A. Kuver, *J. Electroanal. Chem.*, 461(1999) 14.
7. M. F. Mrozek, H. Luo and M.J. Weaver, *Langmuir,* 16 (2000) 8463.
8. M.S. El-Deab, L.A. Kibler and D.M. Kolb, *Electrochem. Commun.*, 11 (2009) 776; M. S. El-Deab, *J. Adv. Research*, 3 (2012) 65.
9. A. Miki, S. Ye, T. Senzaki and M. Osawa, *J. Electroanal. Chem.,* 563 (2004) 23.
10. J.D. Lovi´ c, A.V. Tripkovi´ c, S.L. Gojkovi´ c, K.D. Popovic, D.V. Tripkovic, P. Olszewski and A. Kowal, *J. Electroanal. Chem.,* 581 (2005)294.
11. H. Lee, S. E. Habas, G. A. Somorjai and P. Yang, *J. Am. Chem.Soc.*,130 (2008) 5406.
12. G. Chen, Y. Li, D. Wang, L. Zheng, G. You, C.-J. Zhong, L. Yang, F. Cai, J. Cai and B. H. Chen, *J. Power Sources,* 196 (2011) 8323.
13. G.A. El-Nagar, A.M. Mohammad, M.S. El-Deab and B.E. El-Anadouli, *Electrochim. Acta*, 94 (2013) 62.
14. a) I.M. Al-Akraa, A.M. Mohammad, M.S. El-Deab and B.E. El-Anadouli, *Chem. Lett.*, 40 (2011) 1374; b) I. M. Al-Akraa, A. M. Mohammad, M. S. El-Deab and B. El-Anadouli, Int. *J. Electrochem. Sci.*, 7 (2012) 3939.
15. a) M. S. El-Deab, F. Kitamura and T. Ohsaka, *J. Power Sources,* 229 (2013) 65; b) M. S. El-Deab, F. Kitamura and T. Ohsaka, *J. Electrochem. Soc.*, 160 (2013) F651-F658.
16. T.J. Schmidt, U.A. Paulus, H.A. Gasteiger and R.J. Behm, *J. Electroanal. Chem.,* 508 (2001) 41.
17. a) K. Kobayashi, Y. Oono and M. Hori, *ECS Meeting Abstr*act (2012) p. 1291 MA2012-02; b) B. D. Gould, O.A. Baturina and K. E. Swider-Lyons, *J. Power Sources,* 188 (2009) 89.
18. N.M. Markovic and P.N. Ross, *J. Electroanal. Chem.*, 330 (1992)499.
19. N.M. Markovic, H.A. Gasteiger, B.N. Grgur and P.N. Ross, *J. Electroanal. Chem.,* 467 (1999) 157.
20. V. Stamenkovic, N.M. Markovic and P.N. Ross Jr., *J. Electroanal. Chem.,* 500 (2001) 44.
21. T.J. Schmidt, U.A. Paulus, H.A. Gasteiger and R.J. Behm, *J. Electroanal. Chem.,* 508 (2001) 41.
22. D. V. Tripkovic, D. Strmcnik, D. v. d. Vliet, V. Stamenkovic and N. M. Markovic, The role of anions in surface electrochemistry, *Faraday Discussions* 140 (2009) 25.
23. A. Zolfaghari, B. E. Conway and G. Jerkiewicz, *Electrochim. Acta*, 47 (2002)1173.
24. N. M. Markovic and P. N. Ross, S*urf. Sci. Reports*, 45 (2002) 117.
25. O. M. Magnussen, *Chem. Rev.*, 102 (2002) 679.
26. Z. Ezerskis and Z. Jusys, *Pure Appl. Chem.,*73 (2001)1929.
27. S. Trasatti and O.A. Petrii, *J. Pure Appl. Chem.,* 63 (1991) 711.
28. J. L. Haan and R. I. Masel, *Electrochim. Acta*, 54 (2009) 4073.